



Prospects for $B_{(s)}^0 \rightarrow \pi^0\pi^0, \eta\eta$ modes and corresponding CP asymmetries at CEPC (Tera-Z)

[arXiv:[2208.08327](https://arxiv.org/abs/2208.08327)]

Yuxin Wang, Sébastien, Olivier, Lingfeng Li,
Manqi Ruan, Shanzhen Chen, Yongfeng Zhu

Status of $B_{(s)}^0 \rightarrow \pi^0\pi^0, \eta\eta$

Experimental and theoretical branching ratios (in units of 10^{-6})

Channel	DATA	SCET [1]	QCDF	pQCD
$B^0 \rightarrow \pi^0\pi^0$	1.59 ± 0.26 [2]	$0.84 \pm 0.29 \pm 0.30 \pm 0.19$	$0.30^{+0.46}_{-0.26}$	$0.24^{+0.09}_{-0.07}$
$B_s^0 \rightarrow \pi^0\pi^0$	< 210 [3]	-	$0.13^{+0.05}_{-0.05}$ [10]	$0.21^{+0.10}_{-0.09}$ [5] $0.28^{+0.08+0.04+0.01}_{-0.07-0.05-0.00}$ [4]
$B^0 \rightarrow \eta\eta$	< 1 [6]	$0.69 \pm 0.38 \pm 0.13 \pm 0.58$ $1.0 \pm 0.4 \pm 0.3 \pm 1.4$	$0.32^{+0.13+0.07}_{-0.05-0.06}$ [7] $0.16^{+0.03+0.43+0.09+0.10}_{-0.03-0.18-0.03-0.05}$ [8]	0.067 [9]
$B_s^0 \rightarrow \eta\eta$	< 1500 [3]	$7.1 \pm 6.4 \pm 0.2 \pm 0.8$ $6.4 \pm 6.3 \pm 0.1 \pm 0.7$	$10.9^{+6.3+5.7}_{-4.0-4.2}$ [10]	$10.4^{+4.9}_{-3.4}$ [5]

- Only $B^0 \rightarrow \pi^0\pi^0$ has been observed experimentally
- $B^0 \rightarrow \pi^0\pi^0$
 - Puzzle: discrepancy between experimental and theoretical BR
 - Necessary channel to determine CKM angle alpha
- Charmless two-body hadronic B-meson decay
 - experimentally clean
 - hadron physics, even new physics

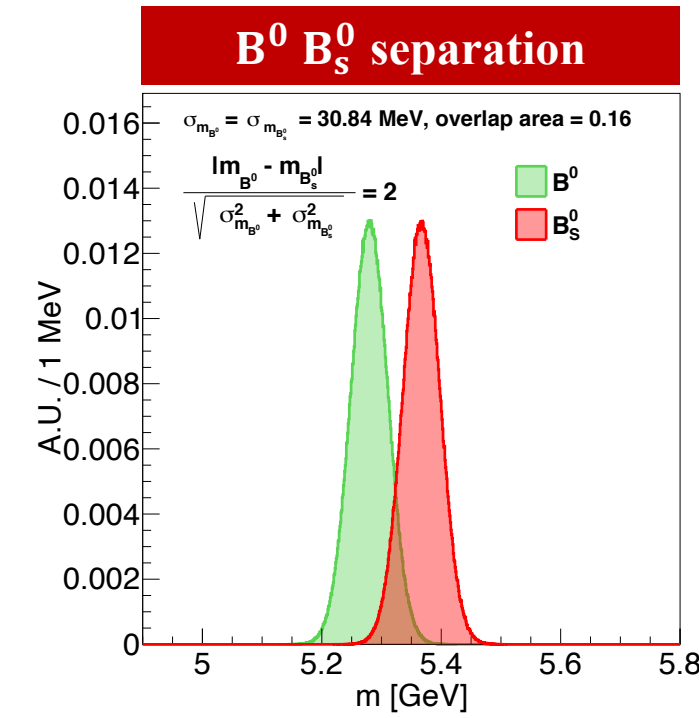
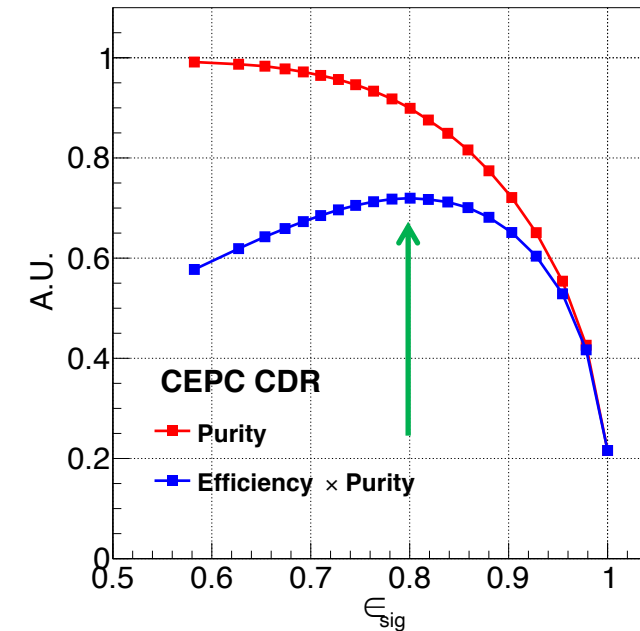
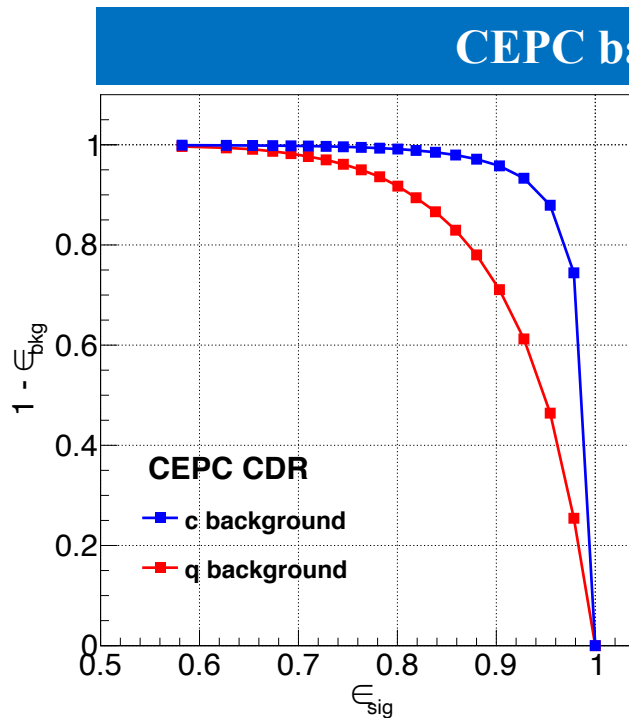
Advantage of CEPC

- Tera-Z factory
 - Massive b-hadrons
 $\sim 10^{11} B^0$ & $\sim 10^{10} B_s^0$
 - Larger boost of b-hadrons than Belle II → more precise vertex reconstruction
- Lepton collider
 - Cleaner collision environment and much lower background level
 - Benefit neutral final states reconstruction

b-hadrons	Belle II	LHCb (300 fb ⁻¹)	Tera-Z
B^0, \bar{B}^0	5.4×10^{10} (50 ab ⁻¹ on $\Upsilon(4S)$)	3×10^{13}	1.2×10^{11}
B^\pm	5.7×10^{10} (50 ab ⁻¹ on $\Upsilon(4S)$)	3×10^{13}	1.2×10^{11}
B_s^0, \bar{B}_s^0	6.0×10^8 (5 ab ⁻¹ on $\Upsilon(5S)$)	1×10^{13}	3.1×10^{10}
B_c^\pm	-	1×10^{11}	1.8×10^8
$\Lambda_b^0, \bar{\Lambda}_b^0$	-	2×10^{13}	2.5×10^{10}

Key detector performance

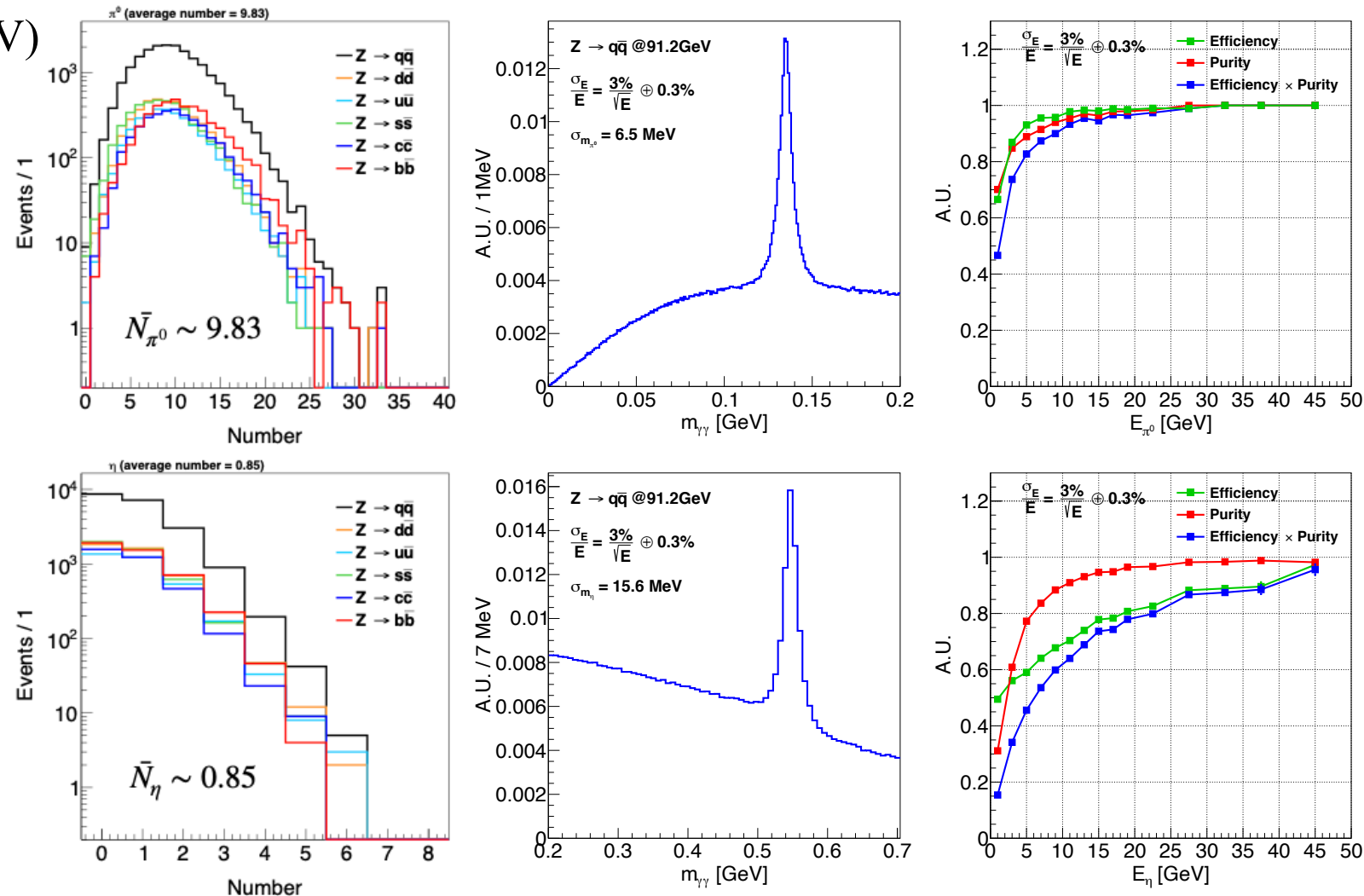
- Fast simulation strategy
- b-jet tagging
 - CEPC baseline: $\varepsilon \sim 80\%$, $p \sim 90\%$
- ECAL performance
 - Only focus on di-photon decay of π^0 and η
 - B mass resolution: $\sigma_{m_B} \sim 30\text{MeV} \rightarrow 2\sigma$ separation between B^0 and B_s^0
 - EM resolution: $3\%/\sqrt{E} \oplus 0.3\%$



Reconstruction performance of π^0 and η

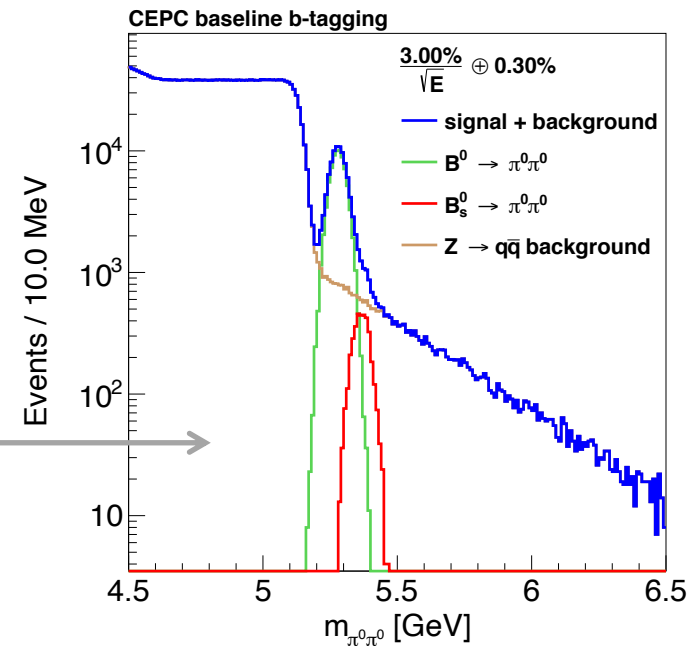
- Inclusive π^0 and η in $Z \rightarrow q\bar{q}$ (91.2 GeV)
 - $\bar{N}_{\pi^0} \gg \bar{N}_\eta$
 - prioritize π^0 reconstruction, use remaining γ to reconstruct η

- Optimal $\epsilon \times p$ vs $E_{\pi^0, \eta}$
 - > 90% for $E_{\pi^0} > 10$ GeV
 - > 60% for $E_\eta > 10$ GeV



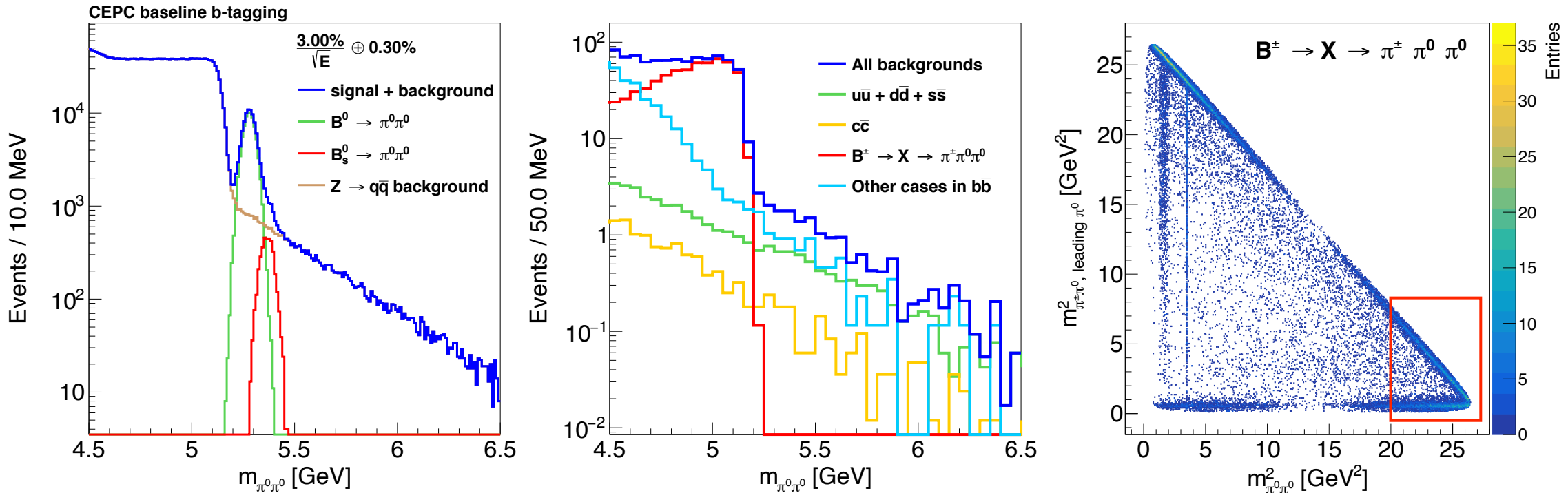
Event selection of $B_{(s)}^0 \rightarrow \pi^0\pi^0$

Selection chain	$B^0 \rightarrow \pi^0\pi^0 \rightarrow 4\gamma$	$B_s^0 \rightarrow \pi^0\pi^0 \rightarrow 4\gamma$	$u\bar{u}+d\bar{d}+s\bar{s}$	$c\bar{c}$	$b\bar{b}$	$\sqrt{S+B}/S$
Yield at Tera-Z	191113	8948	4.29×10^{11} (61.21%)	1.20×10^{11} (17.19%)	1.51×10^{11} (21.60%)	
b-tagging	152890	7159	3.64×10^9 (2.70%)	9.94×10^9 (7.38%)	1.21×10^{11} (89.92%)	
$\pi^0 \rightarrow \gamma\gamma$	148213	6953	3.61×10^9	9.91×10^9	1.21×10^{11}	
Lower $E_{\pi^0} > 6$ GeV	92407	4391	8.44×10^8	1.60×10^9	1.31×10^{10}	
Higher $E_{\pi^0} > 14$ GeV	87355	4142	3.08×10^8	3.15×10^8	1.91×10^9	
$E_{\pi^0\pi^0} > 22$ GeV	87073	4127	2.90×10^8	2.82×10^8	1.66×10^9	
$\theta_{\pi^0\pi^0} < 23^\circ$	77970	3636	1.19×10^8	1.02×10^8	6.04×10^8	
$m_{\pi^0\pi^0} \in (5.212, 5.347)$ GeV	75859	933	5472	1622	8673	$0.40\% \pm 0.01\%$
$m_{\pi^0\pi^0} \in (5.336, 5.397)$ GeV	2831	2545	2424	473	2248	$4.0\% \pm 0.6\%$



- After b-tagging & π^0 reconstruction
- 4 cuts on energy and angular distributions of π^0 pairs
 - Signal efficiency $\sim 40\%$
 - Background suppression ~ 3 orders of magnitude
- Optimize mass window \rightarrow minimize accuracy $\sqrt{S+B}/S$
 - $\sim 7.5 \times 10^4$ $B^0 \rightarrow \pi^0\pi^0$, accuracy $\sim 0.4\%$
 - $\sim 2.5 \times 10^3$ $B_s^0 \rightarrow \pi^0\pi^0$, accuracy $\sim 4.0\%$

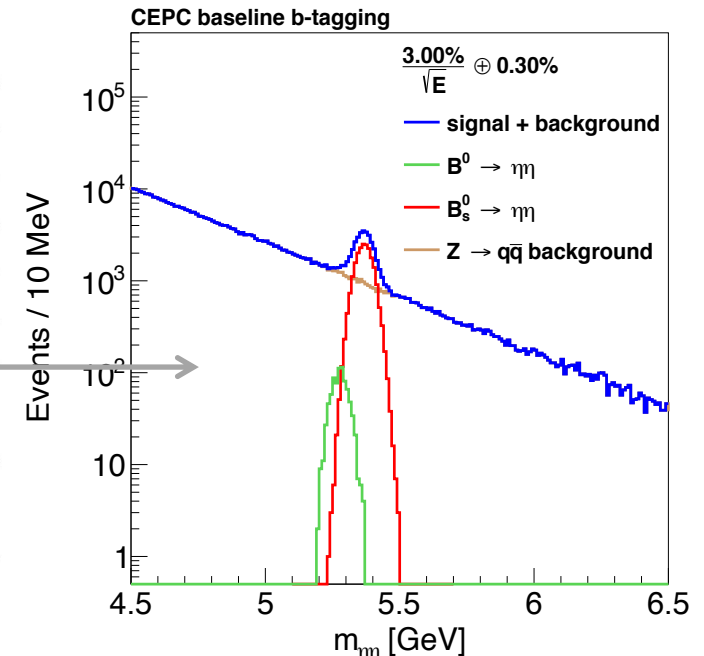
Background components of $B_{(s)}^0 \rightarrow \pi^0\pi^0$



- Step structure mainly from $B^\pm \rightarrow X \rightarrow \pi^\pm\pi^0\pi^0$
 - $m_{\pi^0\pi^0}^2 > 20$ GeV 2
 - $\sim 93\%$ $B^\pm \rightarrow \rho(770)^\pm\pi^0, \rho(770)^\pm \rightarrow \pi^\pm\pi^0$
 - $\sim 7\%$ $B^\pm \rightarrow \pi^\pm\pi^0\pi^0$
 - Kinematic constraint \rightarrow cut-off on $m_{\pi^0\pi^0} \sim 5.2$ GeV

Event selection of $B_{(s)}^0 \rightarrow \eta\eta$

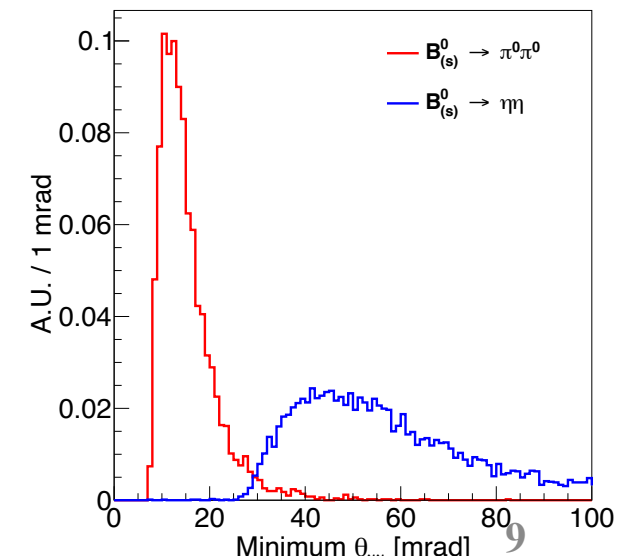
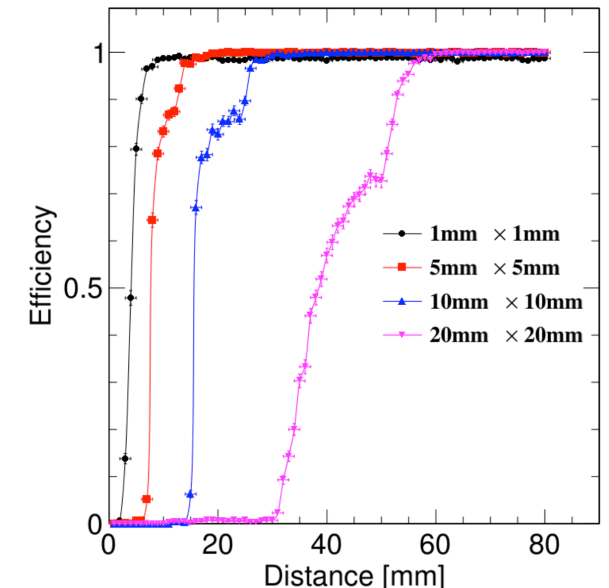
Selection chain	$B^0 \rightarrow \eta\eta \rightarrow 4\gamma$	$B_s^0 \rightarrow \eta\eta \rightarrow 4\gamma$	$u\bar{u} + d\bar{d} + s\bar{s}$	$c\bar{c}$	$b\bar{b}$	$\sqrt{S + B}/S$
Yield at Tera-Z b-tagging	1912 1529	47437 37950	4.29×10^{11} 3.64×10^9	1.20×10^{11} 9.94×10^9	1.51×10^{11} 1.21×10^{11}	
$\eta \rightarrow \gamma\gamma$ $E_{\eta\eta} > 20$ GeV $\theta_{\eta\eta} < 30^\circ$	1000 934 814	25820 24158 21135	2.13×10^8 1.39×10^7 6.76×10^6	5.60×10^8 1.09×10^7 5.68×10^6	9.41×10^9 9.46×10^7 5.17×10^7	
$m_{\eta\eta} \in (5.233, 5.326)$ GeV	693	2103	2328	676	8030	17% $\pm 2\%$
$m_{\eta\eta} \in (5.310, 5.423)$ GeV	155	19208	2184	1014	7388	0.90% $\pm 0.05\%$



- After b-tagging & η reconstruction
- Cuts on energy and angular distributions of η pairs
 - Signal efficiency $\sim 45\%$
 - Background suppression ~ 5 orders of magnitude
- Optimize mass window \rightarrow minimize accuracy $\sqrt{S + B}/S$
 - ~ 700 $B^0 \rightarrow \eta\eta$, accuracy $\sim 17\%$
 - $\sim 2 \times 10^4$ $B_s^0 \rightarrow \eta\eta$, accuracy $\sim 0.9\%$

Other effects

- Photon conversion
 - Central region $\sim 5\text{-}10\%$, Forward region $\sim 25\%$, $\sim 80\%$ can be recovered
 - Average conversion rate $\sim 3\%$ (each photon)
 - $\rightarrow 12\%$ efficiency lost of $B_{(s)}^0 \rightarrow \pi^0\pi^0, \eta\eta$
- Photon separation (especially di-photon merging)
 - 2cm $\rightarrow 80\%$ separation efficiency (CEPC baseline, 5GeV γ)
 - 2cm $\rightarrow 10$ mrad angular separation (ECAL $R_{\text{inner}}=2\text{m}$)
 - Only energetic π^0 suffers
 - $\rightarrow 10\%$ efficiency lost of $B_{(s)}^0 \rightarrow \pi^0\pi^0$



Final realistic results

Channels	$B^0 \rightarrow \pi^0\pi^0$	$B_s^0 \rightarrow \pi^0\pi^0$	$B^0 \rightarrow \eta\eta$	$B_s^0 \rightarrow \eta\eta$
Signal yield	60000	2000	600	17500
Accuracy	0.45%	4.5%	18%	0.95%

Determination of CKM angle α

- CKM matrix: quark mixing, CP violation
- B^0 decay related triangle relation

$$V_{ub}V_{ud}^* + V_{cb}V_{cd}^* + V_{tb}V_{td}^* = 0,$$

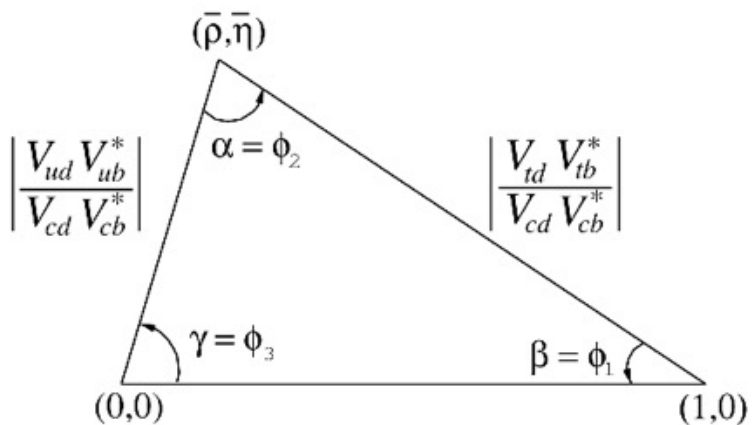


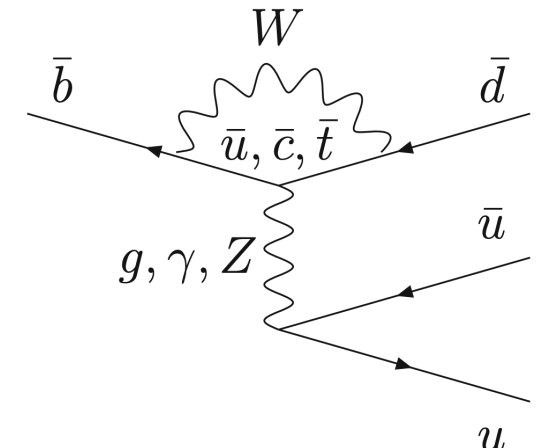
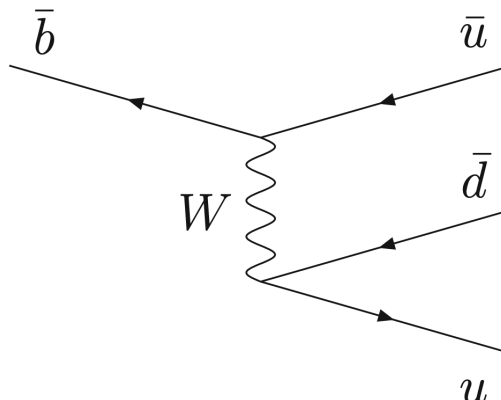
Figure 12.1: Sketch of the unitarity triangle.

$$\beta = \phi_1 = \arg \left(- \frac{V_{cd} V_{cb}^*}{V_{td} V_{tb}^*} \right),$$

$$\alpha = \phi_2 = \arg \left(- \frac{V_{td} V_{tb}^*}{V_{ud} V_{ub}^*} \right),$$

$$\gamma = \phi_3 = \arg \left(- \frac{V_{ud} V_{ub}^*}{V_{cd} V_{cb}^*} \right).$$

- α determination via weak transition $b \rightarrow u\bar{u}$
- Commonly used decay modes
 - $B \rightarrow \rho\rho, \pi\pi, \rho\pi$
- Both tree and penguin diagrams
- Penguin contribution is non-negligible
- Using isospin conservation to deal with penguin pollution



Determination of CKM angle α

Ref. <https://inspirehep.net/literature/1598487>

Isospin analysis of $B \rightarrow \pi \pi$: $B^0 \rightarrow \pi^+ \pi^-$, $\pi^0 \pi^0$, $B^+ \rightarrow \pi^+ \pi^0$

- 3 amplitudes can be parameterized by 12 real parameters (complex tree and penguin contributions)
- 6 parameters can be further eliminated by:
 - 2 complex isospin relations (4 real constraints) \longrightarrow $A^{+0} = \frac{1}{\sqrt{2}} A^{+-} + A^{00}$
 - absence of penguin contribution to $B^+ \rightarrow \pi^+ \pi^0$ (2 real constraints)
- Remain only 6 degrees of freedom!
- From experimental side
 - 6 observables are available to constrain the 6D parameter space
 - \mathcal{B}^{ij} : branching ratio
 - \mathcal{C}^{ij} : direct CP asymmetry in decay
 - \mathcal{S}^{ij} : B - \bar{B} mixing induced CP asymmetry

$$\frac{1}{\tau_{B^{i+j}}} \mathcal{B}^{ij} = \frac{|A^{ij}|^2 + |\bar{A}^{ij}|^2}{2},$$

$$\mathcal{C}^{ij} = \frac{|A^{ij}|^2 - |\bar{A}^{ij}|^2}{|A^{ij}|^2 + |\bar{A}^{ij}|^2},$$

$$\mathcal{S}^{ij} = \frac{2\mathcal{I}m(\bar{A}^{ij} A^{ij*})}{|A^{ij}|^2 + |\bar{A}^{ij}|^2},$$

Current input parameters to determine α

Parameters	World average [30]	Belle (0.8 ab ⁻¹)	Belle II (50 ab ⁻¹) [18]	LHCb
$\mathcal{B}^{00} (\times 10^{-6})$	1.59 ± 0.26 (16%)	1.31 [31] ± 0.19 (14.5%) ± 0.19	1.31 ± 0.03 (2.3%) ± 0.03	-
$\mathcal{B}^{+0} (\times 10^{-6})$	5.5 ± 0.4 (7.3%)	5.86 [59] ± 0.26 (4.4%) ± 0.38	5.86 ± 0.03 (0.6%) ± 0.09	-
$\mathcal{B}^{+-} (\times 10^{-6})$	5.12 ± 0.19 (3.7%)	5.04 [59] ± 0.21 (4.2%) ± 0.18	5.04 ± 0.03 (0.6%) ± 0.08	-
C_{CP}^{00}	-0.33 ± 0.22	-0.14 [31] ± 0.36 ± 0.10	-0.14 ± 0.03 ± 0.01	-
C_{CP}^{+-}				-0.34 ± 0.06 ± 0.01 [61] (7 & 8 TeV, 3.0 fb ⁻¹)
	-0.314 ± 0.030	-0.33 [60] ± 0.06 ± 0.03	-0.33 ± 0.01 ± 0.03	-0.311 ± 0.045 ± 0.015 [62] (13 TeV, 1.9 fb ⁻¹) ± 0.004 (stat. only) [19] (Run 1–6, 300 fb ⁻¹)
S_{CP}^{+-}				-0.63 ± 0.05 ± 0.01 [61] (7 & 8 TeV, 3.0 fb ⁻¹)
	-0.670 ± 0.030	-0.64 [60] ± 0.08 ± 0.03	-0.64 ± 0.01 ± 0.01	-0.706 ± 0.042 ± 0.013 [62] (13 TeV, 1.9 fb ⁻¹) ± 0.004 (stat. only) [19] (Run 1–6, 300 fb ⁻¹)

- No S_{CP}^{00} in current data
 - Lack of vertex information in $B^0 \rightarrow \pi^0\pi^0 \rightarrow 4\gamma$
 - Lead to mirror solutions in α

Complementarity between Z- and B-factory

- Time-integrated CP measurements at Z- and B-factories are quite different but complementary!
 - Z-factory (B from bb pairs, incoherently), $t \in [0, \infty)$, $a_{CP} = C + xS$.
 - B-factory ($\Upsilon \rightarrow BB$, coherently), $t \rightarrow \Delta t \in (-\infty, +\infty)$, $a_{CP} = C$.
- An alternative way to extract S_{CP}^{00} by combining Z- and B-factories

$|q_d/p_d| \simeq 1$ [26]. The time-dependent decay rates become [42–44]:

$$\Gamma_{B^0/\bar{B}^0 \rightarrow f_{CP}}(t) \propto e^{-\Gamma_d t} \left[1 \pm C_{f_{CP}} \cos(\Delta m_d t) \mp S_{f_{CP}} \sin(\Delta m_d t) \right].$$

even
odd

$$C_{f_{CP}} \equiv \frac{1 - |\lambda_{f_{CP}}|^2}{1 + |\lambda_{f_{CP}}|^2}, \quad S_{f_{CP}} \equiv \frac{2 \text{Im} \lambda_{f_{CP}}}{1 + |\lambda_{f_{CP}}|^2}, \quad \lambda_{f_{CP}} \equiv \frac{q_d}{p_d} \frac{\bar{\mathcal{A}}_{f_{CP}}}{\mathcal{A}_{f_{CP}}},$$

$e^{-\Gamma|\Delta t|}$
even

This leads to the definition of the measured time-dependent CP asymmetry:

$$a_{f_{CP}}(t) \equiv \frac{\Gamma_{\bar{B} \rightarrow f_{CP}}(t) - \Gamma_{B \rightarrow f_{CP}}(t)}{\Gamma_{\bar{B} \rightarrow f_{CP}}(t) + \Gamma_{B \rightarrow f_{CP}}(t)} \simeq -C_{f_{CP}} \cos(\Delta m_d t) + S_{f_{CP}} \sin(\Delta m_d t),$$

and the time-integrated CP asymmetry:

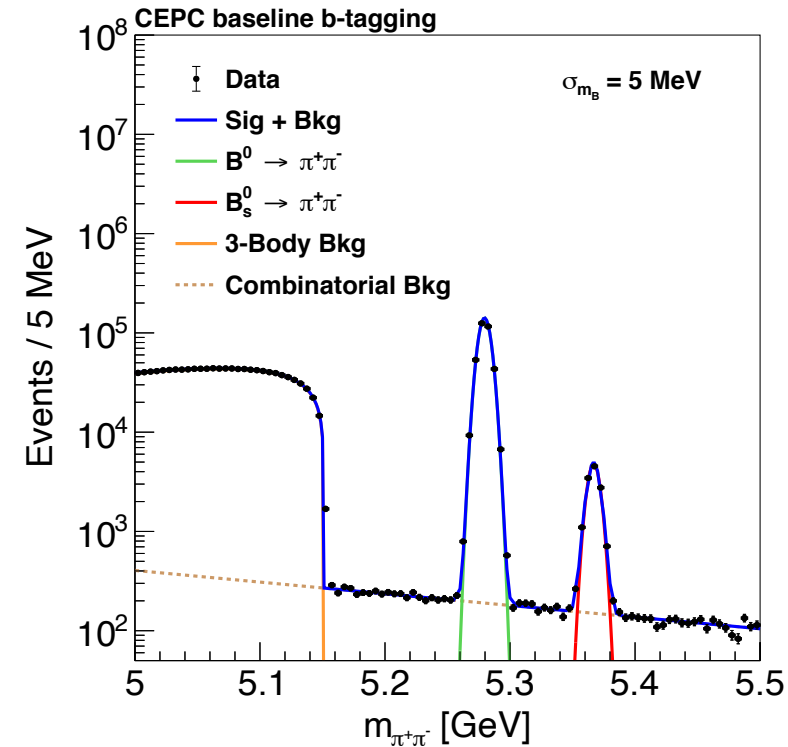
$$a_{f_{CP}} \equiv \frac{\int_0^\infty \Gamma_{\bar{B} \rightarrow f_{CP}}(t) - \Gamma_{B \rightarrow f_{CP}}(t) dt}{\int_0^\infty \Gamma_{\bar{B} \rightarrow f_{CP}}(t) + \Gamma_{B \rightarrow f_{CP}}(t) dt} \simeq \frac{1}{1 + (\Delta m_d/\Gamma_d)^2} \left(-C_{f_{CP}} + S_{f_{CP}} \frac{\Delta m_d}{\Gamma_d} \right).$$

$\int_{-\infty}^\infty$
linear combination

Estimation of other two $B \rightarrow \pi\pi$ modes

- $B^0 \rightarrow \pi^+ \pi^-$ (MCTruth analysis)
 - $E_{\text{tarck}} > 1 \text{ GeV}$
 - $E_{\text{total}} > 20 \text{ GeV}$
 - $\theta < 30^\circ$
 - $|\text{Vertex} - \text{IP}| < 100 \mu\text{m}$
 - Track momentum resolution $\sim 0.1\%$
- $B^+ \rightarrow \pi^+ \pi^0$ (Just a guesswork)
 - Anticipated performance in between 00 and +-
 - Rough estimation using “efficiency & purity”

$$\frac{\sigma_B}{B} \simeq \frac{1}{\sqrt{N_{\text{eff}}}} \equiv \frac{1}{\sqrt{\text{Yield} \times \epsilon \times p}}$$



Channel	Branching ratio $B (\times 10^{-6})$	Yield at Tera-Z	Efficiency ϵ	Purity p	$\epsilon \times p$	σ_B/B
$B^0 \rightarrow \pi^0 \pi^0$	1.59	1.9×10^5	32%	80%	25%	0.45%
$B^+ \rightarrow \pi^+ \pi^0$	5.50	6.6×10^5	50%	$\gtrsim 85\%$	43%	0.19%
$B^0 \rightarrow \pi^+ \pi^-$	5.12	6.1×10^5	55%	$\gtrsim 95\%$	52%	0.18%

CP asymmetries of $B \rightarrow \pi\pi$

- Uncertainty estimation (only statistical)

$$\sigma_{a_{CP}^{00}} \simeq \frac{1}{(1 - 2\chi_d)\sqrt{N_{\text{eff}} \times \epsilon_{\text{eff}}}} \text{ (time-integrated)}$$

$$\sigma_{S_{CP}^{+-}} \simeq \sigma_{C_{CP}^{+-}} \simeq \frac{1}{\sqrt{N_{\text{eff}} \times \epsilon_{\text{eff}}}} \text{ (time-dependent)}$$

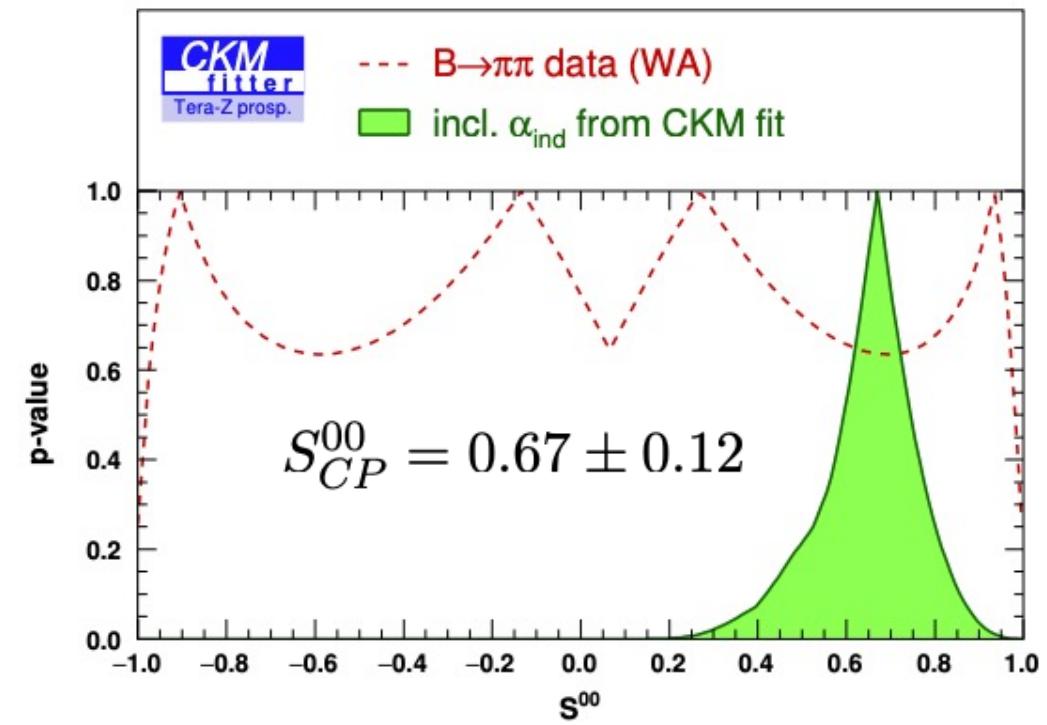
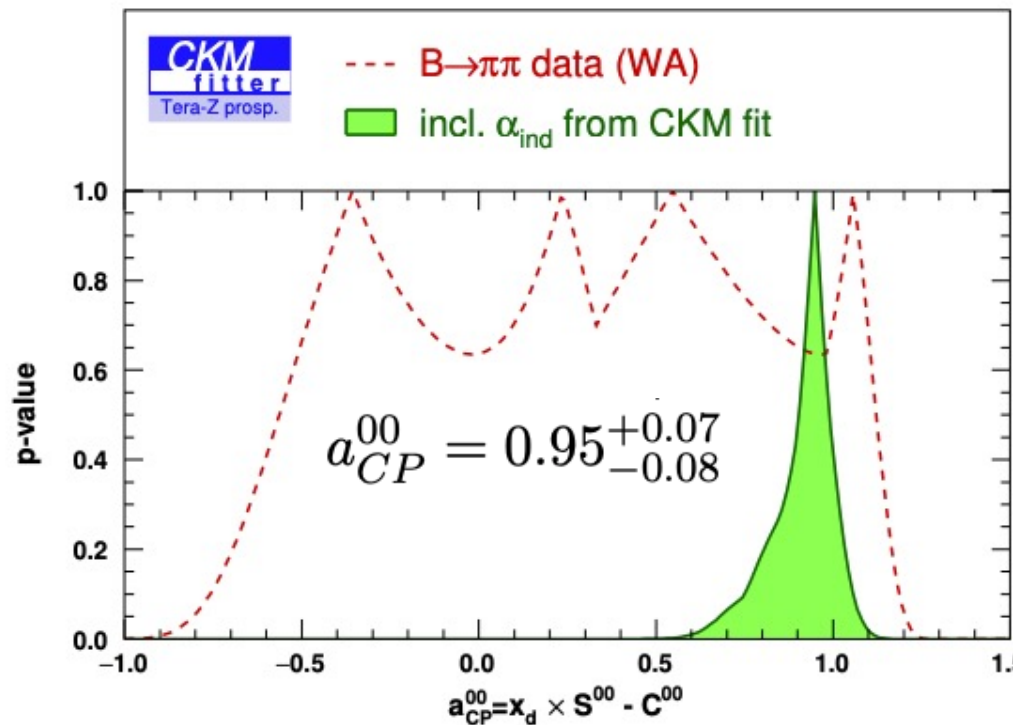
- b-charge tagging (B^0 or \bar{B}^0):
 - effective tagging efficiency (power), ϵ_{eff}
 - $\epsilon_{\text{eff}} \equiv \epsilon_{\text{tag}}(1 - 2\omega)^2 \in [15, 25]\%$
 - tagging efficiency, ϵ_{tag}
 - wrong tag fraction, ω
- B^0 - \bar{B}^0 mixing: $\chi_d = 0.1858 \pm 0.0011$

Parameters	Tera-Z Projection
$\sigma_{\mathcal{B}^{00}}/\mathcal{B}^{00}$	0.45%
$\sigma_{\mathcal{B}^{+0}}/\mathcal{B}^{+0}$	0.19%
$\sigma_{\mathcal{B}^{+-}}/\mathcal{B}^{+-}$	0.18%
$\sigma_{a_{CP}^{00}}$	$\pm (0.014\text{--}0.018)$
$\sigma_{C_{CP}^{+-}}$	$\pm (0.004\text{--}0.005)$
$\sigma_{S_{CP}^{+-}}$	$\pm (0.004\text{--}0.005)$

CKM global fit

by Sébastien & Olivier (CKMfitter group)

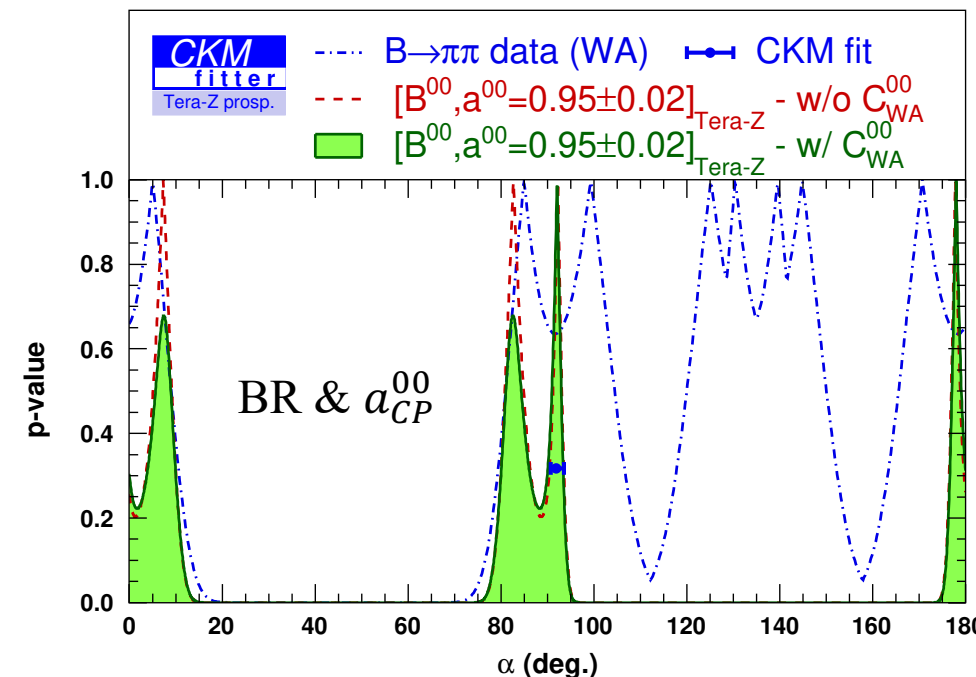
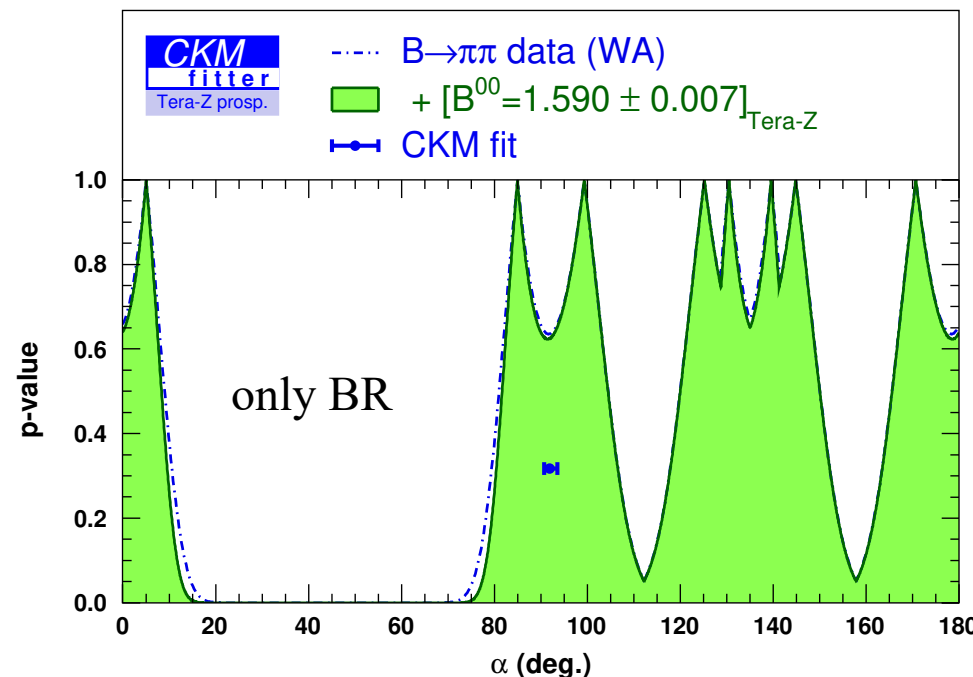
- Uncertainties rescaled to the Tera-Z projections
- The choice of central value
 - a_{CP}^{00} and S_{CP}^{00} , current predictions of the CKM global fit
 - Others, keep to the W.A.



CKM global fit

- Scenario 1: only improve $B^0 \rightarrow \pi^0\pi^0$ to Tera-Z projection
 - Left: only improve BR
 - Right: improve both BR & a_{CP}^{00}
 - Main improvement comes from a_{CP}^{00}
 - Some mirror solutions removed by $a_{CP}^{00} = C + xS$ at Tera-Z
 - Final precision of α : $2\sim 3^\circ$ (with additional C_{WA}^{00} from B-factories)

WA : $\alpha(\pi\pi) = (93.0 \pm 13.6)^\circ \rightarrow$ Tera-Z scenario 1 : $\alpha(\pi\pi) = (82.6_{-2.5}^{+3.5} \cup 92.0_{-2.0}^{+1.4})^\circ$



CKM global fit

- Scenario 2: improve all three $B \rightarrow \pi\pi$ modes to Tera-Z projection

➤ a_{CP}^{00} and C_{CP}^{00} are central in this improvement

➤ Final precision of α :

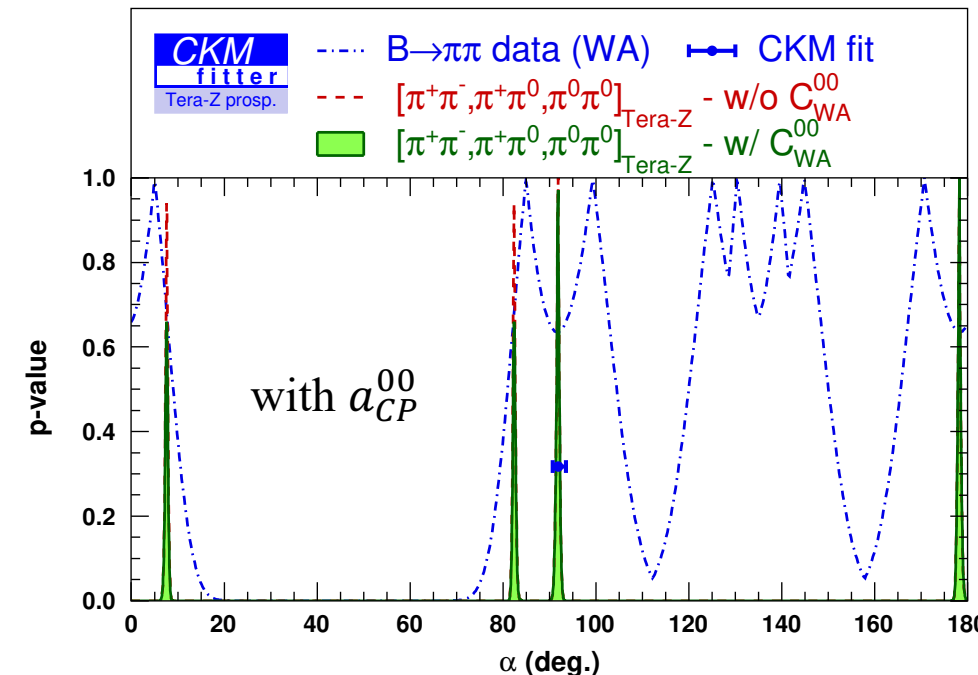
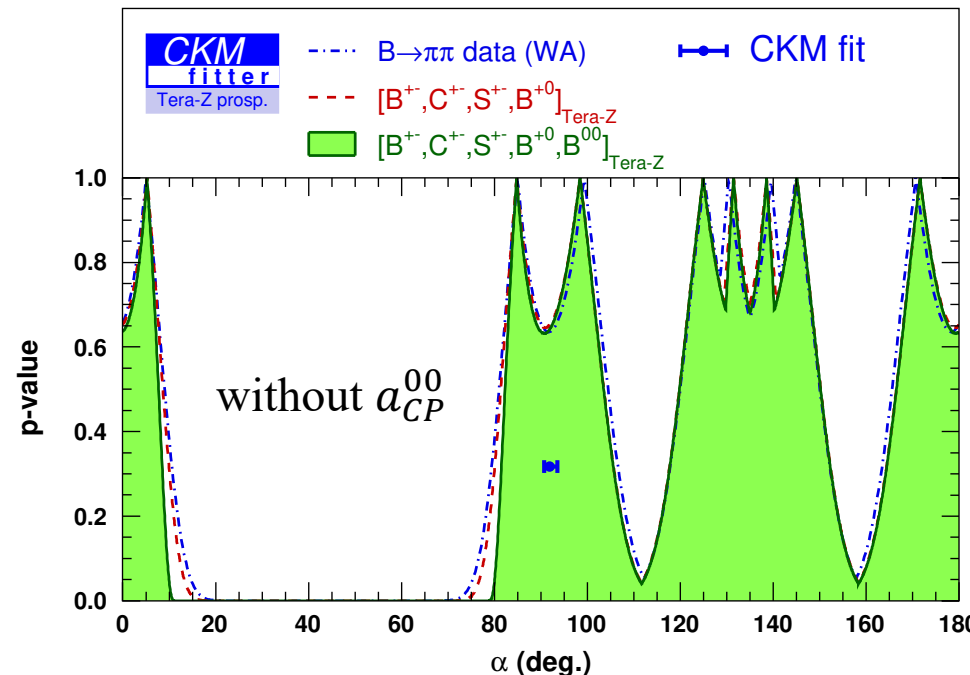
$$\text{Tera-Z scenario 2 : } \alpha(\pi\pi) = (91.8 \pm 0.4)^\circ$$

- Need to emphasize:

➤ Central values matter a lot.

➤ Other values can be seen in [arXiv:[2208.08327](https://arxiv.org/abs/2208.08327)]

➤ Theoretical systematic uncertainties (isospin related) $\sim 1\text{-}2^\circ$, need to reevaluate



Other prospects for α measurement

- Direct extraction of $S_{\pi\pi}^{00}$ via time-dependent analysis of $B^0 \rightarrow \pi^0\pi^0$
 - Using $\pi^0 \rightarrow e^+e^-\gamma$ Dalitz decay or photon conversion events
 - CEPC advantage
 - Larger boost of B meson
 - Decent vertex reconstruction
 - B decay lifetime resolution ~ 15 fs
- $B \rightarrow \rho\rho$, more precise than $B \rightarrow \pi\pi$ modes
 - Larger branching ratios than $B \rightarrow \pi\pi$
 - $B^0 \rightarrow \rho^0\rho^0$ enjoys the charged final state $\rho^0 \rightarrow \pi^+\pi^-$
 - Much better charged particle reconstruction performance than neutral particle
 - $S_{\rho\rho}^{00}$ is available to reduce the mirror solutions in α

Summary

- Neutral charmless B-meson decays: $B_{(s)}^0 \rightarrow \pi^0\pi^0, \eta\eta$
 - Fast simulation: key detector performance modeling
 - CEPC baseline b-tagging: $\varepsilon \sim 80\%$, $p \sim 90\%$
 - EM resolution: $3\%/\sqrt{E} \oplus 0.3\%$ ($\sigma_{m_B} \sim 30\text{MeV}$)
 - Other effects: photon conversion & separation
 - Anticipated accuracy at Tera-Z →

- CKM angle α determination using $B \rightarrow \pi\pi$ mode
 - Complementarity between Z- and B-factory in
 - extracting S_{CP}^{00}
 - reducing mirror solutions in α
 - Anticipated precisions of $B \rightarrow \pi\pi$ BR & CP asymmetries →
 - CKM global fit results
 - Only improve $B^0 \rightarrow \pi^0\pi^0$: $\sigma(\alpha) \approx 2\text{--}3^\circ$
 - Improve all three $B \rightarrow \pi\pi$: $\sigma(\alpha) \approx 0.4^\circ$
 - Central value matters!
 - Prospects
 - Reevaluation of theoretical systematic uncertainties
 - Direct extraction of $S_{\pi\pi}^{00}$ via π^0 Dalitz decay or photon conversion
 - More precise measurement of $B \rightarrow \rho\rho$

Channels	$B^0 \rightarrow \pi^0\pi^0$	$B_s^0 \rightarrow \pi^0\pi^0$	$B^0 \rightarrow \eta\eta$	$B_s^0 \rightarrow \eta\eta$
Signal yield	60000	2000	600	17500
Accuracy	0.45%	4.5%	18%	0.95%

Parameters	Tera-Z Projection
$\sigma_{\mathcal{B}^{00}}/\mathcal{B}^{00}$	0.45%
$\sigma_{\mathcal{B}^{+0}}/\mathcal{B}^{+0}$	0.19%
$\sigma_{\mathcal{B}^{+-}}/\mathcal{B}^{+-}$	0.18%
$\sigma_{a_{CP}^{00}}$	$\pm (0.014\text{--}0.018)$
$\sigma_{C_{CP}^{+-}}$	$\pm (0.004\text{--}0.005)$
$\sigma_{S_{CP}^{+-}}$	$\pm (0.004\text{--}0.005)$

Thank you!

b-charge tagging (jet charge measurement)

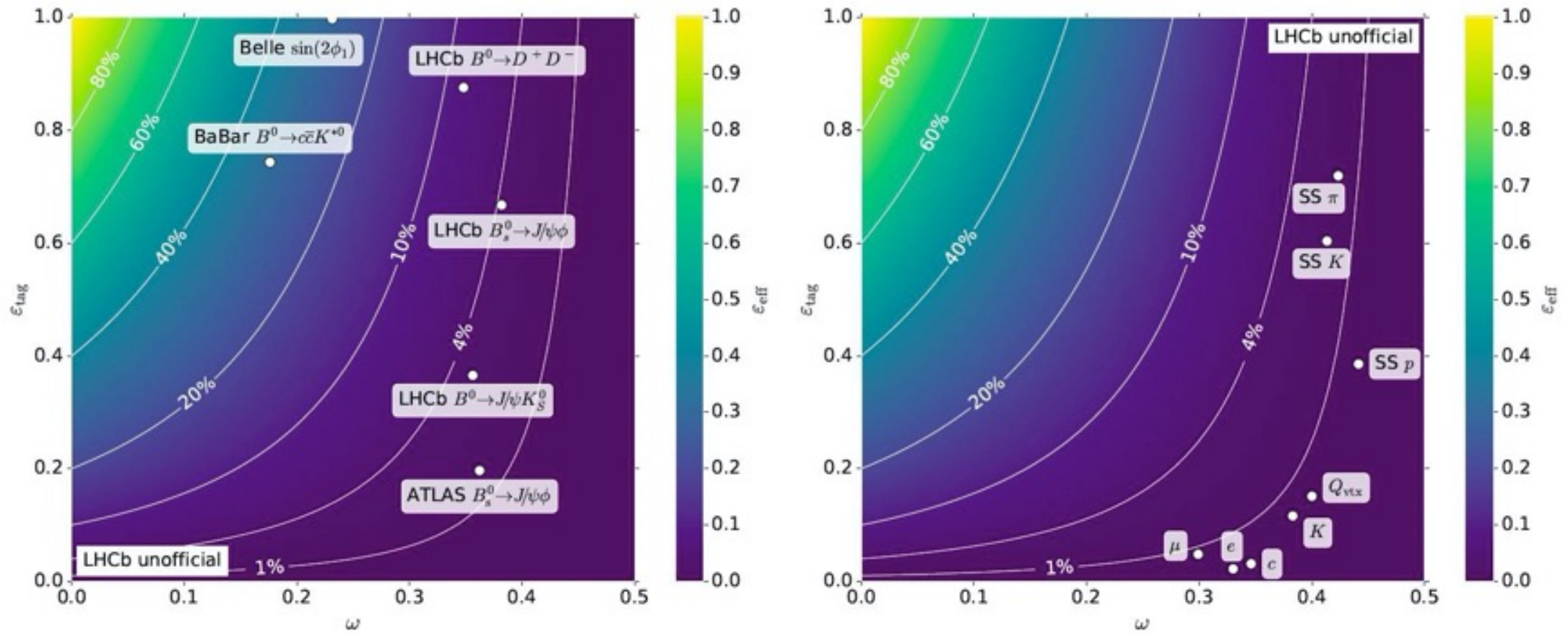


Figure 3.1: Effective tagging efficiency of (left) different HEP experiments and (right) LHCb flavour tagging algorithms [40]. The white lines indicate contours of constant tagging power.

b-charge tagging (jet charge measurement)

- b-charge tagging performance:

- wrong tag fraction, ω
- tagging efficiency, ϵ_{tag}
- effective tagging efficiency (power), ϵ_{eff}

$$\epsilon_{eff} = \epsilon_{tag}(1 - 2\omega)^2$$

- b-charge tagging at CEPC

- Jet charge measurement at MCTruth level (by Hanhua)

- infer b-charge by leading charged particles
 - $\omega \sim 35\%$, $\epsilon_{eff} \sim 10\%$

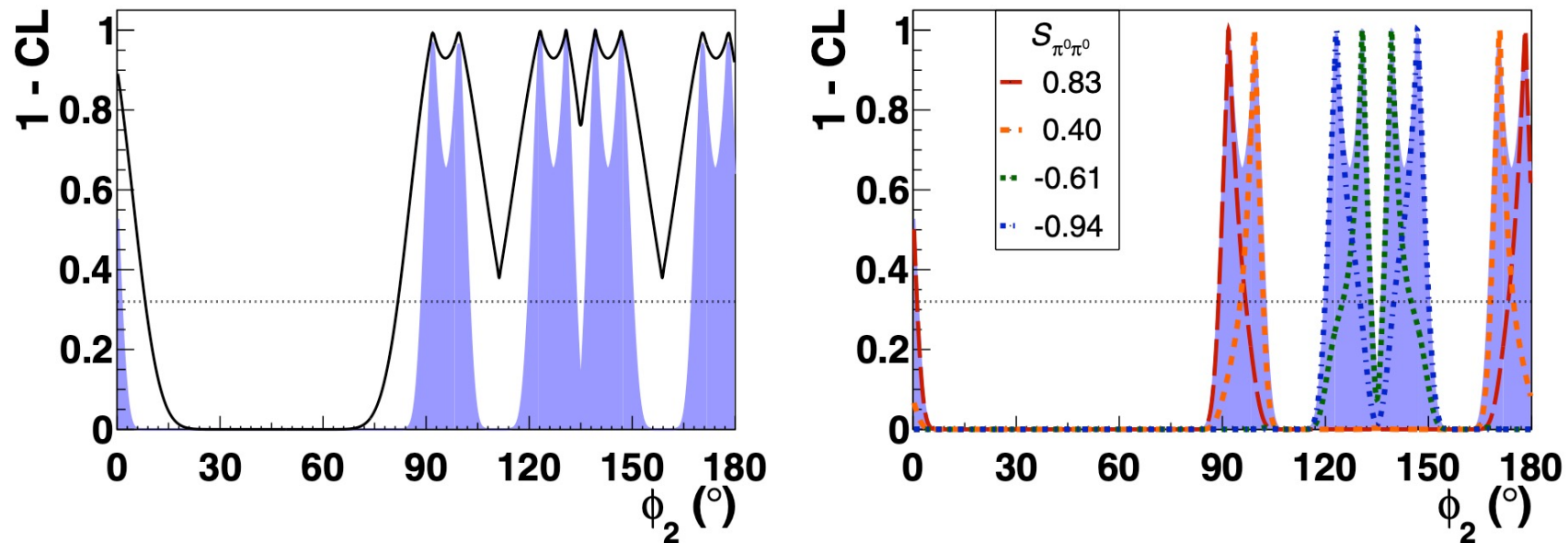
- Dedicated b-charge tagging algorithm for $B_s \rightarrow J/\psi\phi$ (by Mingrui)

- potential to improve $\omega \sim 25\%$, $\epsilon_{eff} \sim 20\%$

$$\begin{aligned} A_{CP}^{Measured} &= \frac{[\bar{N}(1 - \omega) + N\omega] - [\bar{N}\omega + N(1 - \omega)]}{\bar{N} + N} \\ &= (1 - 2\omega) \frac{\bar{N} - N}{\bar{N} + N} = (1 - 2\omega) A_{CP}^{Truth} \end{aligned}$$

Time-dependent CP asymmetry of $B^0 \rightarrow \pi^0\pi^0$: $S_{\pi\pi}^{00}$

- Extra constraint of $S_{\pi\pi}^{00}$ can reduce the two-fold ambiguity on the solutions of α in $[75, 105]^\circ$
- Time-dependent analysis need vertex information
 - $\pi^0 \rightarrow e^+e^-\gamma$ Dalitz decay or photon conversion events
 - Belle II: 147 Dalitz events & 124 photon conversion events



- CEPC advantage
 - Larger boost of B meson
 - Decent vertex reconstruction
 - B decay lifetime resolution ~ 15 fs

More precise determination of α using $B \rightarrow \rho \rho$

- More precise than $B \rightarrow \pi \pi$ modes
 - Larger branching ratios than $B \rightarrow \pi \pi$
 - $B^0 \rightarrow \rho^0 \rho^0$ enjoys the charged final state $\rho^0 \rightarrow \pi^+ \pi^-$
 - Much better charged particle reconstruction performance than neutral particle
 - $S_{\rho\rho}^{00}$ is accessible to reduce the ambiguity solutions

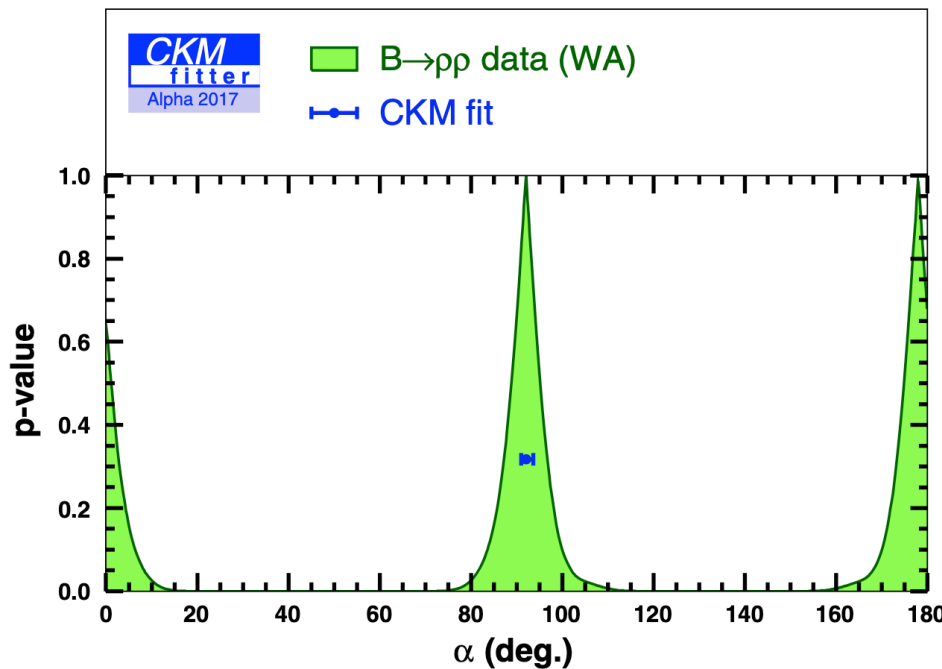


Table 4 World averages for the relevant experimental observables in the $B \rightarrow \rho^i \rho^j$ modes: branching fraction $\mathcal{B}_{\rho\rho}^{ij}$, fraction of longitudinal polarisation f_L^{ij} , time-integrated CP asymmetry $\mathcal{C}_{\rho\rho}^{ij}$, time-dependent asymmetry $\mathcal{S}_{\rho\rho}^{ij}$ and correlation (ρ)

Observable	World average
$\mathcal{B}_{\rho\rho}^{+-} \times f_L^{+-} (\times 10^6)$	$(27.76 \pm 1.84) \times (0.990 \pm 0.020)$
$\mathcal{B}_{\rho\rho}^{+0} \times f_L^{+0} (\times 10^6)$	$(24.9 \pm 1.9) \times (0.950 \pm 0.016)$
$\mathcal{B}_{\rho\rho}^{00} \times f_L^{00} (\times 10^6)$	$(0.93 \pm 0.14) \times (0.71 \pm 0.06)$
$\mathcal{C}_{\rho_L \rho_L}^{+-}$	-0.00 ± 0.09
$\mathcal{S}_{\rho_L \rho_L}^{+-}$	-0.15 ± 0.13
$\rho(C_{\rho_L \rho_L}^{+-}, S_{\rho_L \rho_L}^{+-})$	$+0.0002$
$\mathcal{C}_{\rho_L \rho_L}^{00}$	0.2 ± 0.9
$\mathcal{S}_{\rho_L \rho_L}^{00}$	0.3 ± 0.7

Table 90. Statistical uncertainties $\Delta A_{\pi^0\pi^0}$, $\Delta S_{\pi^0\pi^0}$, and $\Delta \mathcal{B}_{\pi^0\pi^0}/\mathcal{B}_{\pi^0\pi^0}$ for different input values of $A_{\pi^0\pi^0}$ and $S_{\pi^0\pi^0}$ used for the generation of signal MC.

Input values		Time-dependent		Time-integrated	
$A_{\pi^0\pi^0}$	$S_{\pi^0\pi^0}$	$\Delta A_{\pi^0\pi^0}$	$\Delta S_{\pi^0\pi^0}$	$\Delta A_{\pi^0\pi^0}$	$\Delta \mathcal{B}_{\pi^0\pi^0}/\mathcal{B}_{\pi^0\pi^0}$ [%]
0.34 [650]	0.65 [650]	0.22	0.28	0.03	2.2
0.43 [88]	0.79	0.23	0.29	0.03	2.2
0.14 [712]	0.83	0.21	0.26	0.03	2.4
0.14 [712]	0.40	0.20	0.29	0.03	2.3
0.14 [712]	-0.61	0.22	0.27	0.03	2.3
0.14 [712]	-0.94	0.22	0.28	0.03	2.4

Table 91. Branching fractions and CP asymmetry parameters entering in the isospin analysis of the $B \rightarrow \pi\pi$ system: Belle measurements at 0.8 ab^{-1} together with the expected Belle II sensitivity at 50 ab^{-1} .

	Value	0.8 ab^{-1}	50 ab^{-1}
$\mathcal{B}_{\pi^+\pi^-} [10^{-6}]$	5.04	$\pm 0.21 \pm 0.18$ [727]	$\pm 0.03 \pm 0.08$
$\mathcal{B}_{\pi^0\pi^0} [10^{-6}]$	1.31	$\pm 0.19 \pm 0.19$ [712]	$\pm 0.03 \pm 0.03$
$\mathcal{B}_{\pi^+\pi^0} [10^{-6}]$	5.86	$\pm 0.26 \pm 0.38$ [727]	$\pm 0.03 \pm 0.09$
$A_{\pi^+\pi^-}$	0.33	$\pm 0.06 \pm 0.03$ [728]	$\pm 0.01 \pm 0.03$
$S_{\pi^+\pi^-}$	-0.64	$\pm 0.08 \pm 0.03$ [728]	$\pm 0.01 \pm 0.01$
$A_{\pi^0\pi^0}$	0.14	$\pm 0.36 \pm 0.10$ [712]	$\pm 0.03 \pm 0.01$

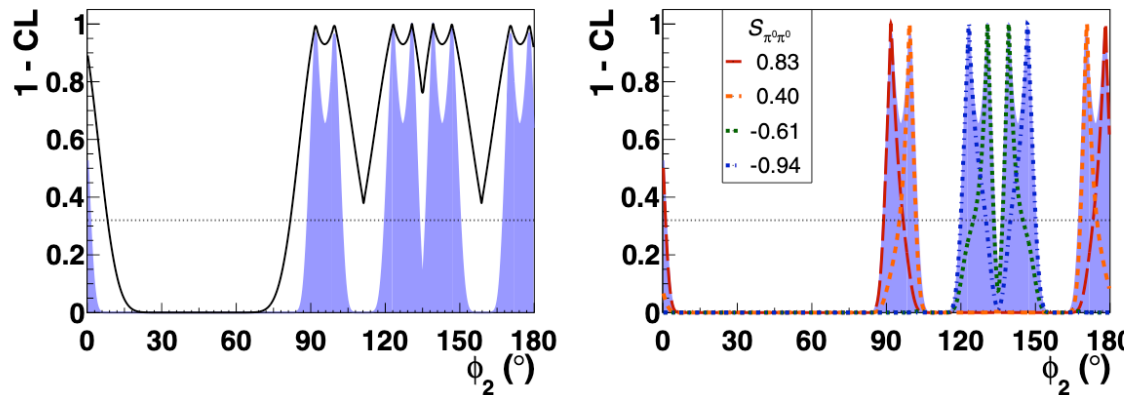


Fig. 116. Scan of the confidence for ϕ_2 performing isospin analysis of the $B \rightarrow \pi\pi$ system. (Left): The black solid line shows the result of the scan using data from Belle measurements (see Table 91). The blue shaded area in both plots shows the projection for Belle II. (Right): Results of the scan adding the $S_{\pi^0\pi^0}$ constraint. Each line shows the result for a different $S_{\pi^0\pi^0}$ value. The dotted horizontal lines correspond to 1σ .

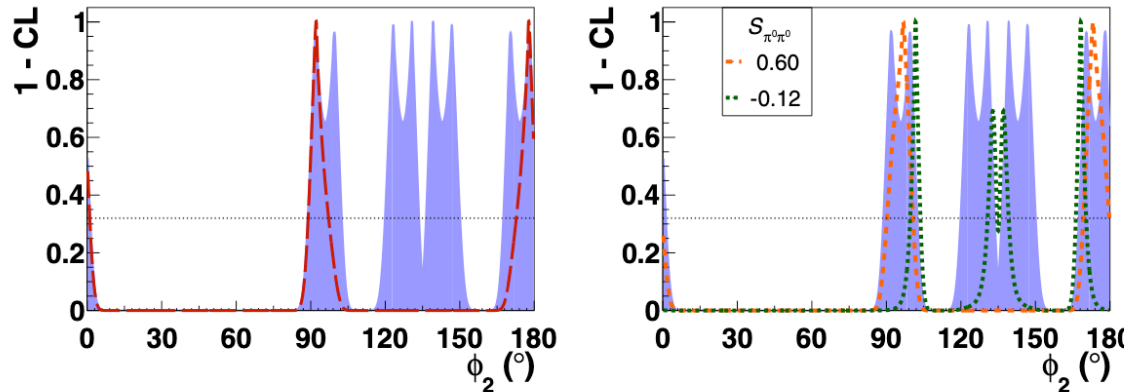
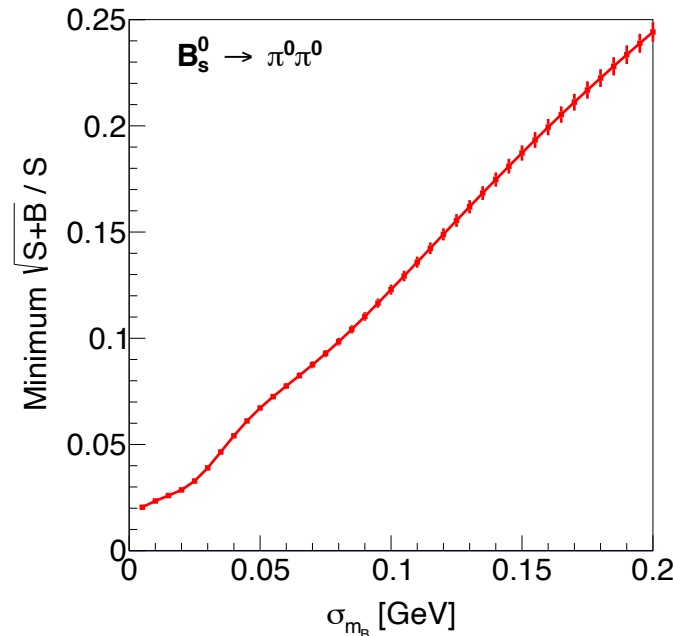
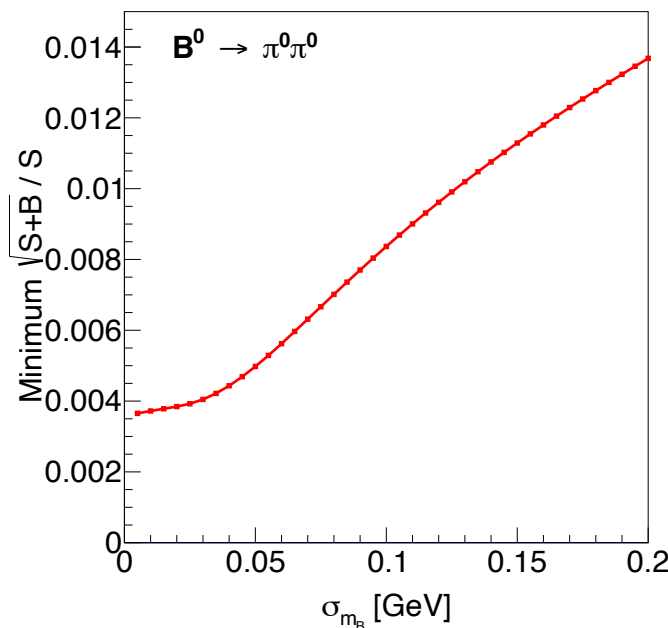


Fig. 117. Scan of the confidence for ϕ_2 performing isospin analysis of the $B \rightarrow \pi\pi$ system. The blue shaded area in both plots shows the projection of the Belle measurements (see Fig. 116) for Belle II. Results of the scan with additional $S_{\pi^0\pi^0}$ constraints are shown by dashed lines. Each line corresponds to different input $S_{\pi^0\pi^0}$ values. The red long dashed line on the left figure shows the result for $S_{\pi^0\pi^0} = 0.83$. The dotted horizontal line corresponds to 1σ .

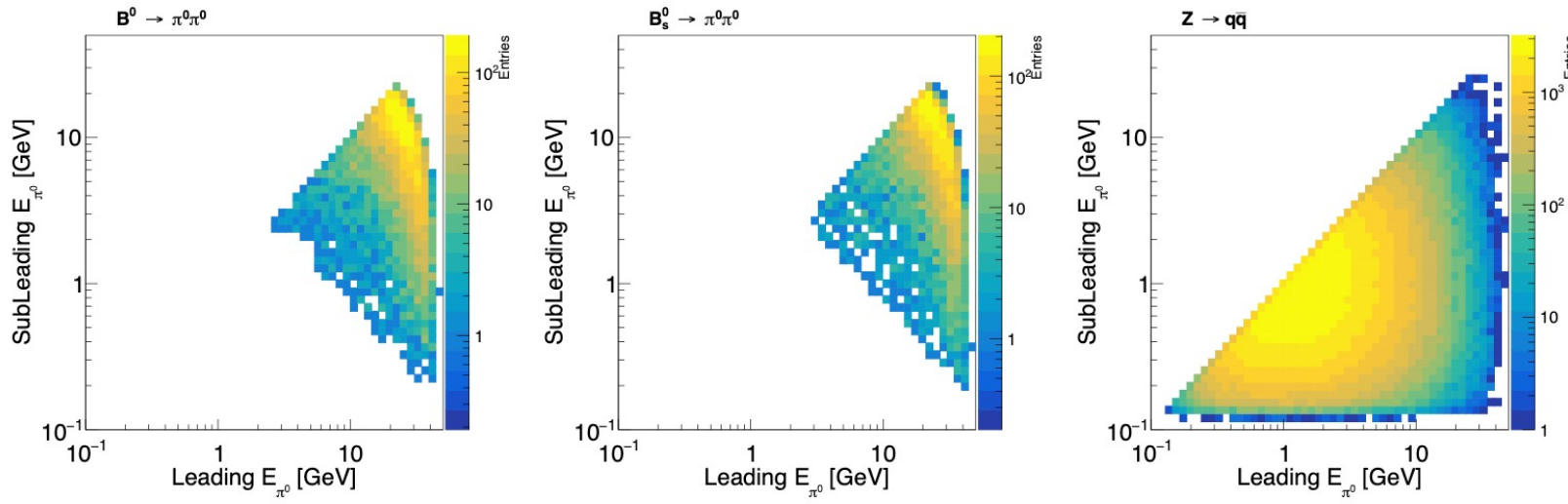
$B^0 \rightarrow \pi^0 \pi^0$	Final state	Total in theory	In acceptance	Selected	Efficiency	Purity	Relative accuracy
Tera-Z	$\pi\pi$	195692	-	-	-	-	-
	$\pi_{\gamma\gamma}\pi_{\gamma\gamma}$	$191113 * 0.65 = 124223$	-	75859 49689	0.4	0.8 0.72	0.4% 0.5%
	$\pi_{dal}\pi_{\gamma\gamma}$	4579	-	?	?		
	$\pi_{cy}\pi_{\gamma\gamma}$	$191113 * 0.2 = 38222$	-	?	?		
Belle II	$\pi\pi$	103000	-	-	-	-	-
	$\pi_{\gamma\gamma}\pi_{\gamma\gamma}$	$100590 - 9270 = 91320$	78486	15068	0.192	0.158	2%
	$\pi_{dal}\pi_{\gamma\gamma}$	2410	2060	147	0.072		0.176
	$\pi_{cy}\pi_{\gamma\gamma}$	$100590 * 0.09 = 9270$	3090	124	0.042		

$\pi_{\gamma\gamma}^0$ are used for the time-integrated CP violation study. There is no event overlap between events with B_{sig}^0 candidates reconstructed from two $\pi_{\gamma\gamma}^0$ and events containing Dalitz decays or converted photons.

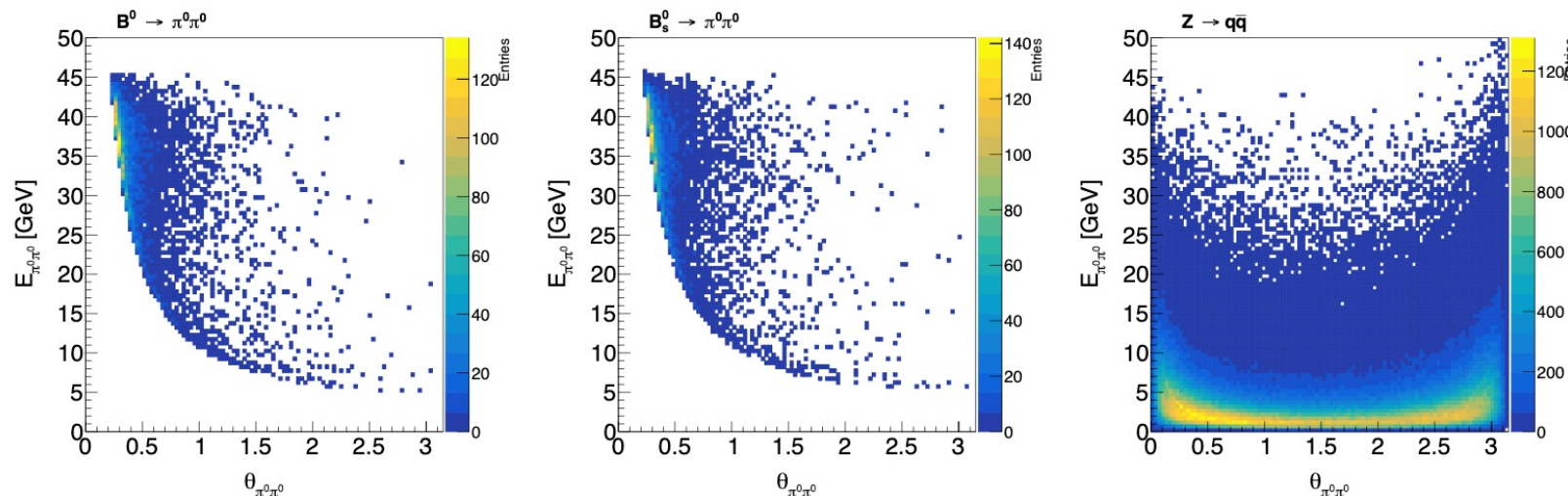


ECAL energy resolution	Channel	σ_{m_B} (MeV)	Signal	$q\bar{q}$ background	Background with false $\pi^0(\eta)$	$\sqrt{S+B}/S$ (%)
$\frac{3\%}{\sqrt{E}} \oplus 0.3\%$	$B^0 \rightarrow \pi^0\pi^0$	30.25	75859	15767	7.52%	0.40 ± 0.01
	$B_s^0 \rightarrow \pi^0\pi^0$	30.21	2545	5145	14.73%	4.03 ± 0.55
	$B^0 \rightarrow \eta\eta$	33.30	693	11034	52.86%	17 ± 2
	$B_s^0 \rightarrow \eta\eta$	33.26	19208	10586	65.25%	0.90 ± 0.05
$\frac{17\%}{\sqrt{E}} \oplus 1\%$	$B^0 \rightarrow \pi^0\pi^0$	166	57746	381331	4.04%	1.15 ± 0.03
	$B_s^0 \rightarrow \pi^0\pi^0$	165	2243	142716	5.74%	19.3 ± 0.6
	$B^0 \rightarrow \eta\eta$	170	324	68243	88.27%	85 ± 6
	$B_s^0 \rightarrow \eta\eta$	174	8300	49248	86.30%	2.90 ± 0.20

Table 8: Measurement accuracies of $B_{(s)}^0 \rightarrow \pi^0\pi^0$ and $B_{(s)}^0 \rightarrow \eta\eta$ at different ECAL energy resolutions when using the CEPC baseline b-tagging.



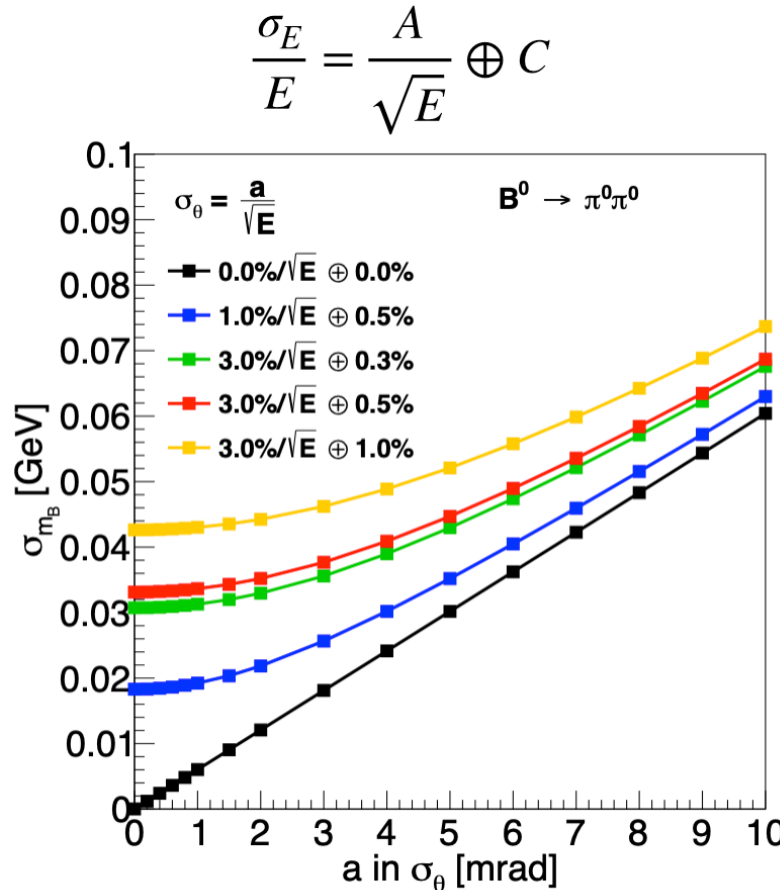
(a) 2D energy spectrum of π^0 pairs in $B^0 \rightarrow \pi^0\pi^0$ (left), $B_s^0 \rightarrow \pi^0\pi^0$ (middle), and $Z \rightarrow q\bar{q}$ (right) events.



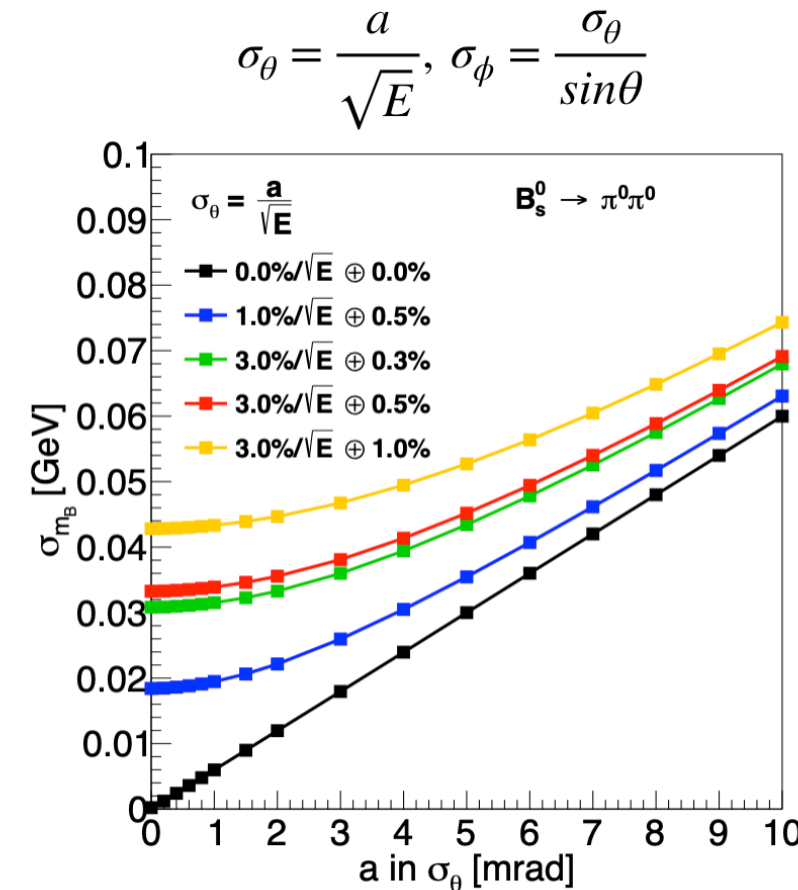
(b) Correlation between $E_{\pi^0\pi^0}$ and $\theta_{\pi^0\pi^0}$ in $B^0 \rightarrow \pi^0\pi^0$ (left), $B_s^0 \rightarrow \pi^0\pi^0$ (middle), and $Z \rightarrow q\bar{q}$ (right) events.

Dependence of B mass resolution on detector performance

ECAL energy resolution



Photon angular resolution

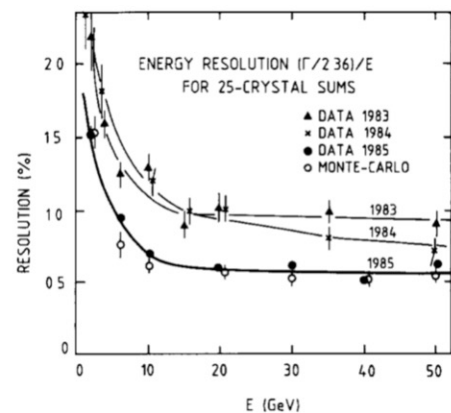
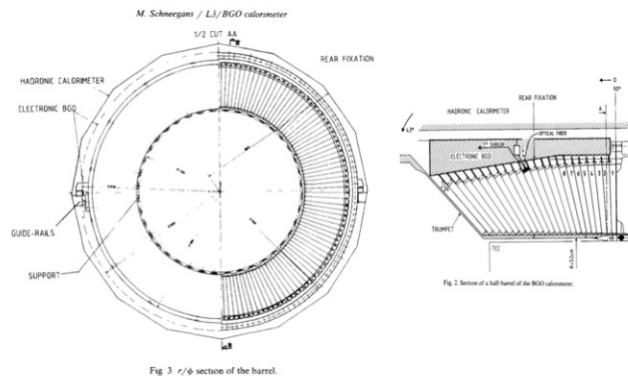


- CEPC baseline single photon angular resolution $\sim 1\text{mrad}/\sqrt{E}$
- ECAL energy resolution dominates the contribution when $\sigma_{\theta} < 1\text{mrad}/\sqrt{E}$
- The following analysis only takes ECAL energy resolution into account
- $\sigma_{mB} \sim 30 \text{ MeV}$ requires ECAL energy resolution $\sim 3\%/\sqrt{E} \oplus 0.3\%$

EM Energy Resolution

From a historical perspective

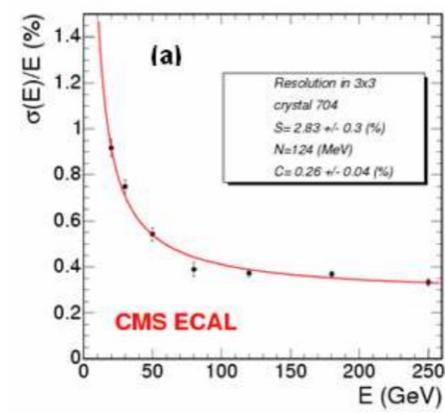
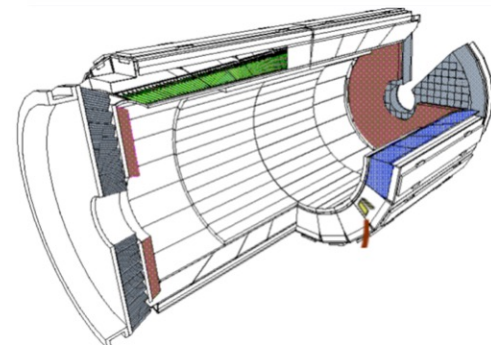
LEP - L3, BGO



< 2% at 1GeV

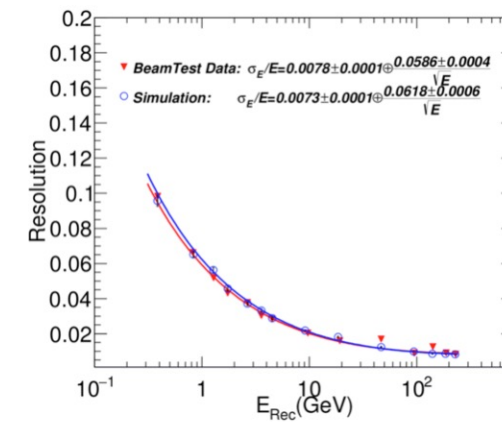
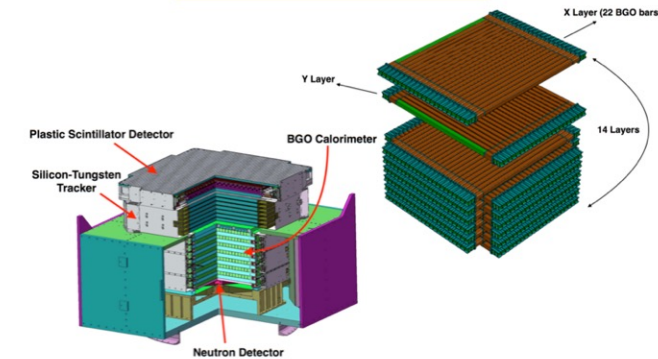
The performance now measured in electron beams with final prototypes shows that we are below 2% energy resolution at 1 GeV and near to 5% at 100 MeV.

LHC - CMS, PbWO4



2.8%/ \sqrt{E} \oplus 0.3%

DAMPE, BGO



5.86%/ \sqrt{E} \oplus 0.78%

Belle II ECAL

The intrinsic energy resolution of the calorimeter, as measured in a prototype [3], can be approximated as:

$$\frac{\sigma_E}{E} = \sqrt{\left(\frac{0.066\%}{E}\right)^2 + \left(\frac{0.81\%}{\sqrt[4]{E}}\right)^2 + (1.34\%)^2}, \quad (9.1)$$

where E is in GeV and the first term represents the electronics noise contribution.

3.5. *Electromagnetic calorimeter (ECL)*

The electromagnetic calorimeter is used to detect gamma rays as well as to identify electrons, i.e. separate electrons from hadrons, in particular pions. It is a highly segmented array of thallium-doped caesium iodide CsI(Tl) crystals assembled in a projective geometry (Fig. 3). All three detector regions, the barrel as well as the forward and backward endcaps, are instrumented with a total of 8736 crystals, covering about 90% of the solid angle in the centre-of-mass system. The CsI(Tl) crystals, preamplifiers, and support structures have been reused from Belle, whereas the readout electronics and reconstruction software have been upgraded. In the Belle experiment, the energy resolution observed with the same calorimeter was $\sigma_E/E = 4\%$ at 100 MeV, 1.6% at 8 GeV, and the angular resolution was 13 mrad (3 mrad) at low (high) energies; π^0 mass resolution was 4.5 MeV/ c^2 [2]; in the absence of background a very similar performance would also be expected for Belle II.